DETERMINATION OF LINEAR VISCOELASTIC MATERIAL PROPERTIES OF PAPER FOR WEB MECHANICS IN PRINTING PRESSES

by

J. O. Lif[1], S. Ostlund[2] and C. Fellers
Swedish Pulp and Paper Research Institute
[1]also Stora Corporate Research
[2]also Royal Institute of Technology
Sweden

ABSTRACT

Analysis of multispan web handling systems such as printing presses requires that viscoelasticity is considered. Guided by the plane and anisotropic nature of paper webs and the relatively small strain levels in a printing press suggests the use of a two dimensional anisotropic linear viscoelastic constitutive model for a first order analysis of the web behavior.

In the present paper a novel procedure for determination of the material functions in such a model, based upon biaxial measurements during small uniaxial sinusoidal excitations of paper strips symmetrically around zero stress, was presented. The drawbacks of buckling of the paper strip during the compressive part of the load cycle was avoided by supporting the paper specimen between glass plates. The method enables in-plane viscoelastic characterization of paper grades in the frequency range 0.000238-10 Hz. The experimental set-up was tested for newsprint and paperboard. The results showed that the method offers the determination of the material functions during a steady-state response which is not the case in conventional set-ups using a static pre-strain in order to avoid buckling.

The experimental data were used for determination of appropriate material functions. The usefulness of the material model was verified by comparing model simulations with different driving stimuli in a tensile tester. The time dependent transverse strain response of paper due to stress relaxation was demonstrated. The comparison between model and experiments indicated that newsprint and paperboard exhibit some non-linear material behavior at the strain amplitude of 0.075 % chosen for obtaining the material parameters. The linear viscoelastic model described the Behaviour of the tested papers within the requirements of engineering accuracy for strain levels typical for many printing applications.

INTRODUCTION

It is commonly known that runnability problems can be avoided by having a uniform web tension on the printing press. A uniform web tension is influenced by disturbances created from reel changes, the vibrational characteristics of wound paper rolls, uneven mechanical properties or even the geometry of the web. The sources of these disturbances results from both the storage and manufacturing of the paper. Other disturbances are produced by the press itself such as imperfections of the parts in the transmission, the gap in the printing cylinder and variations in the ink and water transfer at the printing units.

During passage through the press, the web is subjected to different types of time dependent mechanical loading and exposed to dampening from water. This results in a moisture and load dependent state of deformation giving history dependent dimensional changes. In order to thoroughly analyze this situation, paper must be regarded as a time dependent hygroscopic material and the press running conditions must be considered. The influence of the mechanical loading, environmental effects and external disturbances on runnability problems such as misregister during multi-color printing, waves, web breaks, wrinkles and web flutter is not well known. During the printing of newspaper, the understanding of the mechanics of web transport is also of great interest when several paper webs enter the folding unit. A recent study investigated the performance of multi web spans in web handling systems and showed the importance of the viscoelasticity of the webs [1]. In order to advance and at least quantitatively understand the influence of the time dependence of the paper web on some of these phenomena, multiaxial mechanical models are needed. In the literature there exists some suggestions of constitutive models of paper. Few have been experimentally verified [2, 3]. Only a few studies have tried to examine viscoelasticity of paper at small strains. Except for ultrasonic measurements, in-plane material data from dynamic testing of paper at small strains seems to be lacking.

The aim of this investigation was to examine a novel experimental setup for the determination of the in-plane viscoelasticity of paper during stationary conditions and compare experiments and model simulations for different types of loading stimulus.

MATERIALS AND METHODS

A multiaxial generalization of the well known convolution integral to describe linear viscoelastic behavior can be done by using a fourth order retardance tensor $U_{ijkl}(t)$, [4], yielding

$$\varepsilon_{ij}(t) = \int_0^t U_{ijkl}(t-\tau)\sigma_{kl}(\tau)d\tau\,, \tag{1}$$

where the Latin indices take on the values 1 to 3 and the summation convention applies. Here $t-\tau$ is the elapsed time since each unit impulse stimuli of the stress tensor σ_{ij} was activated and ε_{ij} is the infinitesimal strain tensor. Laplace transformation of Eq. (1) allows the utilization of the simplicity afforded by the Laplace transformed constitutive model

$$\tilde{\varepsilon}_{ij}(s) = \tilde{U}_{ijkl}(s)\cdot\tilde{\sigma}_{kl}(s)\,. \tag{2}$$

In Eq. (2), the tilde character denotes the corresponding transformed functions and s is the transform variable. Here, the 1- and 2-directions lie in the plane of the web and corresponds to the machine (MD) and cross (CD) directions respectively. The 3-direction corresponds to the thickness direction (ZD). Assuming a plane state of stress and taking into account the symmetries of the stress and strain tensors and material symmetries, five unknown material functions remain in Eq. (2). In matrix notation we have

$$\begin{bmatrix} \tilde{\varepsilon}_{11} \\ \tilde{\varepsilon}_{22} \\ \tilde{\gamma}_{12} \end{bmatrix} = \begin{bmatrix} \tilde{U}_{11} & \tilde{U}_{12} & 0 \\ \tilde{U}_{21} & \tilde{U}_{22} & 0 \\ 0 & 0 & \tilde{U}_{66} \end{bmatrix} \begin{bmatrix} \tilde{\sigma}_{11} \\ \tilde{\sigma}_{22} \\ \tilde{\tau}_{12} \end{bmatrix}. \tag{3}$$

It is assumed that the material symmetries are parallel to the 1-2 coordinate axes. Experiments with harmonic excitation of paper strips at several frequencies can be used to find discrete data to the unknown material functions in Eq. (3). The details of this procedure are described in [5].

The functions $\tilde{U}ij$ have the dimension of compliance and are usually denoted as the complex compliances J_{ij}^*. The interconversion between compliance and stiffness within the frequency domain is straight forward [4]. The relations connecting the complex stiffnesses and the complex compliances are in matrix notation

$$\mathbf{G}^*(\omega) \cdot \mathbf{J}^*(\omega) = \mathbf{I}, \tag{4}$$

where $\mathbf{I}$ is the unit matrix. Thus, $\mathbf{G}^*(\omega)$ is the reciprocal of $\mathbf{J}^*(\omega)$.

Four functions are to be determined if the symmetry $\tilde{U}_{12} = \tilde{U}_{21}$ of the material in Eq. (3) is assumed to be valid. To preserve the symmetry in the complex matrices, i.e. $J_{12}^* = J_{21}^*$ and $G_{12}^* = G_{21}^*$, the necessary condition is $\delta_{12} = \delta_{21}$, where δ_{12} and δ_{21} are the coupled loss angles. A reasonable assumption of δ_{12} is

$$\delta_{12} = \delta_{21} = (\delta_{11} + \delta_{22}) / 2. \tag{5}$$

The so-called dissipation factors or the specific losses [4] are here given by

$$\tan \delta^*_{\alpha\beta} = -\frac{J''_{\alpha\beta}(\omega)}{J'_{\alpha\beta}(\omega)} \text{ or } \tan \delta^{**}_{\alpha\beta} = \frac{G''_{\alpha\beta}(\omega)}{G'_{\alpha\beta}(\omega)}, \tag{6}$$

where the single and the double prime superscripts denote the real and the imaginary parts of the corresponding complex functions respectively. These are the well known storage and loss properties of the material [4]. The loss angles in Eq. (6) can be found to fulfill the condition $\delta_{\alpha\beta} = \delta^*_{\alpha\beta} = \delta^{**}_{\alpha\beta}$ only if Eq. (5) holds.

All that remains is the evaluation of the shear compliance $\tilde{U}_{66}(s)$. This property is determined during harmonic tensile testing of paper strips at an off-axis direction with regards to the material principal directions. For simplicity, the well known point transformation rules of compliances is used.

If it is assumed that paper behaves like a standard model [4], each component of the transformed retardance matrix in Eq. (3) can be written as a transformed generalized Kelvin model

$$\widetilde{U}(s) = J_g + \sum_{i=1}^{N} \frac{J_i}{1+\tau_i \cdot s} + \{\phi / s\} . \tag{7}$$

In Eq. (7) the compliance spectrum lines and the corresponding retardation times are denoted by J_i and τ_i, and ϕ is the steady-flow fluidity included only if steady-state flow is modeled. Equation (7) is used by Akatsuka [6], with only one term in the sum to model paper webs. The generalized Maxwell model

$$\underset{\sim}{Q}(s) = G_g - \sum_{i=1}^{N} \frac{G_i}{1+\tau_i \cdot s} \tag{8}$$

is the conjugate model to Eq. (7) and describes the relaxance of the material. The time independent term G_g is the glassy modulus.

<u>**Generating model parameters from harmonic responses**</u>

The Fourier transformed Kelvin model can at a stationary condition be obtained by the substitution $s = i\omega$ in the retardance $\widetilde{U}(s)$ in Eq. (7). The real and imaginary parts of that model are given by

$$J'(\omega) = J_g + \sum_{i=1}^{N} \frac{1}{1+\tau_i^2 \omega^2} \text{ and } J''(\omega) - \{\phi / \omega\} = \sum_{i=1}^{N} J_i \frac{\tau_i \cdot \omega}{1+\tau_i^2 \cdot \omega^2} \tag{9}$$

The functions in the sums of Eqs. (9) are the kernels which can be used in the iterative algorithm of Tschoegl and Emri [7-10], referred to subsequently as the TE-algorithm, to model the storage and loss compliance.

The TE-algorithm has been implemented in Matlab. An interpolation routine was used to estimate data between experimental source data. The source data of newsprint and paperboard are reported in [5]. The measurements were run in displacement control where the loss and storage modulii material properties were obtained. The source data describing the loss and storage compliances was obtained by utilizing the Fourier transformed version of the reciprocal relation, Eq. (4), on the experimentally determined complex modulii. The TE-algorithm, using either the loss or the storage kernels, was then used on compliance source data to obtain compliance line spectras. The modulii line spectras were obtained using the storage kernel in Eq. (9) on storage modulii source data. Since the source data only covered a limited frequency window, the instantaneous viscoelastic constants J_g, and G_g were approximated at a selected cut-off frequency. The range of frequencies tested were not enough to approximate the steady flow term ϕ from the modulus line spectra [4]. This term was neglected throughout this work.

Paper strips were subjected to different loading stimuli in order to investigate the performance of the anisotropic model. Their exists both tension and velocity controlled parts of the web transport in the printing process. This may cause different types of transient phenomena in paper, such as creep and relaxation, and influenced the shape of the test program.

Idealized boundary conditions were assumed when loading in the MD of the papers. Furthermore, it was assumed that the material was at rest at time zero and that boundaries perpendicular to the loading direction were stress free.

First of all, creep and creep recovery was investigated. An illustration of the load history is given in Fig. 2a. The condition during the relaxation test was obtained by superimposing a new constant strain rate to reach a strain level constant in time after one second. Finally, a strain deformation history shown in Fig. 2b was used. The constant strain rates in this loading history were of the order of $5.0 \cdot 10^{-5}$ and $1.7 \cdot 10^{-5} s^{-1}$.

EXPERIMENTAL PROCEDURE

After a couple of cycles of sinusoidal strain, the transient arising from the initial condition is negligible when the testing is performed without the superimposed static tensile strain. A condition without static strain can be achieved by supporting the test piece with plates, particularly useful during the compressive part of the stress-strain cycle. This idea was used for the design of an in-plane deformation tester to be installed in a MTS 448.00 servo hydraulic tensile tester. The system is illustrated in Fig. 1. Glass plates were used as they have low surface roughness, can be made parallel and secures ocular inspections during testing. The back glass plate was adjustable at three points to become parallel to the clamps after mounting in the tester. A vertical clearance of 0.5 mm in the 1-direction between the clamps and the glass plates was considered enough to avoid buckling of the test piece near the clamps when a compressive longitudinal stress was imposed on the test piece. The front plate was adjusted by two micrometers in the 1-3 plane to become parallel to the back plate. The micrometers were also used to change the horizontal clearance between the paper test piece and the plates. The top clamp could not rotate in the 2-3 plane and was always parallel to the bottom clamp. This eliminated any influence from twisting during the experiments. The low weight bottom clamp reduced the inertial effects at higher frequencies.

MTS low force fatigue load cells, 50 and 1000 N, were used, the longitudinal strain signal was compensated for the deformation of the cell during testing. The use of conventional strain gauges for the estimation of the strains, within the rectangular test piece, which was 50 by 200 mm, greatly simplified data acquisition. The 1-directional strain, the position of the top clamp was recorded during cyclic testing by an eddy current gauge. The average longitudinal strain within the test piece must equal the displacement of the top clamp divided by the clamped length. This was found within the experimental error as reported in [5].

In the 2-direction, i.e. the transverse direction, the position of a modified clip-on gauge MTS model 832.11c-22 was adjusted by a 1-3 table positioned by micrometers. A rod was used to link the gauge to the table. During testing the rod may be regarded as simply supported. As a result, the clip-on was free to move in the test piece plane at small displacements. During mounting, the strip was held between the two plates. With this, the strip was correctly clamped for even stress distribution. Needles (diam. 0.4 mm), separated by 40 mm, mounted on the gauge arms penetrated the test piece after this moment. The transverse motion of the needles were then used to evaluate the transverse strains.

Two papers typical for sheet and web fed offset printing were used. An uncoated solid bleached sulfate board (200 g/m^2) with a moisture content of 6.6% and a thickness of 255 ±8 μm. The newsprint (45 g/m^2) was composed of 84% thermomechanical, 11% groundwood and 5% softwood pulps, moisture content of 8.1% and a thickness of 60 ±3 μm. Standard uniaxial tensile tests were performed on paperboard according to the SCAN-P67 testing method. The tensile stiffness index was 9.36 in MD and 3.86 MNm/kg in CD. The coefficient of variation (COV) was 2% on the paperboard stiffnesses. The tensile stiffness index on newsprint were 9.27 in MD and 1.81 MNm/kg in CD with a COV of 3% and 4% respectively. Stiffness index as well as modulii in this paper was expressed in terms of force per grammage and width, i.e. MNm/kg. All experiments were performed at 23° C and 50% RH.

The major weakness with the proposed setup, the influence from frictional heating during slippage between the glass plates and the paper test piece on the evaluated material properties was investigated. Extensive measurements and adjustments of the plates position with regard to the clamped 1-3 plane were performed on test pieces loaded in MD or CD. Above a clearance of 0.03 mm no influence on the evaluated viscoelastic properties was observed. At increasing clearance, the loop became asymmetric. This is demonstrated in Fig. 3 where the specific stress response, including the start-up phase of paper test pieces, at low frequency displacement controlled sinusoidal excitation is shown. When the newsprint test piece was subjected to compressive stresses, small longitudinal buckles of the strip could be observed ocularly through the plates at large clearances. This was also found to be the reason for the asymmetry of the loop, since increasing clearance was found to increase the asymmetry. The undesirable thickness to width ratio and the low stiffness of the test piece was claimed to give rise for the buckling phenomenon. This is also illustrated by the improved performance of the paperboard test piece in Fig. 3. Newsprint loaded in the MD also showed less asymmetric behavior. The load signal from newsprint loaded in CD is not easily analyzed when the test piece enters the compressive part as illustrated in Fig. 3. However, a steady state response is demonstrated on both newsprint and paperboard. From these findings it was decided to disregard the compressive part of the load signal in the evaluation of the viscoelastic properties. Analyzing the load signal in this way $\tan\delta$ above the clearance 0.04 mm reaches a plateau value and becomes independent of the positioning [5].

When testing at the plateau levels of G' and $\tan\delta$, we were not able to examine the transverse strain amplitudes and the loss angles $\tan\delta_{\alpha\beta}$ in a indisputable manner. In order to achieve an acceptable linear relation between the transverse and longitudinal strains, we had to decrease the clearance to about 0.01 to 0.02 mm between the plates and the test piece. Unfortunately, under these conditions, the magnitude of the measured coupled loss angles decreased systematically. Thus, the measured coupled loss angles was not regarded as material properties and could not be used in the analysis. However the storage properties was not significantly affected at these clearances. A possible motion between the holes and the needles within the test piece was found negligible after comparing results before and after running long cyclic tests at 10 Hz and clearance of 0.02 mm. It was decided to evaluate the longitudinal amplitudes and the longitudinal loss angles from experiments without the clip-on gauge mounted. A total horizontal clearance of 0.05 mm symmetrical with regard to the test piece was selected for further trials using only the tensile part of the load signal. Additional experiments were then performed to evaluate the in-plane strain peak amplitudes, $\hat{\varepsilon}_{11}$ and, $\hat{\varepsilon}_{22}$ at clearances of about 0.01 to 0.02 mm. The computed signal-to-noise ratio at this condition was of the same order as that found on the oscilloscope indicating excellent experimental conditions.

Since all equations were based on linear behavior of the material, the linearity of the paper grades needed to be examined. For this purpose test pieces loaded in CD preferably can be used since the CD shows a more pronounced nonlinearity. The outcome was used to select the displacement amplitudes since the cyclic tests were run in displacement control. Large amplitudes yield higher accuracy since the signal-to-noise ratios are improved in the measurement system. After this, three replicate experiments on test pieces loaded in MD, CD, and 45° were performed to obtain the in-plane complex modulii at the outlined conditions. Each test piece was run in a non systematic order; 12 harmonic cycles at the frequencies 0.000236 to 0.01 Hz; and 25 harmonic cycles at 0.1 to 10 Hz respectively.

RESULTS

The linear viscoelastic behavior of the tested papers was examined by varying the strain amplitude and the amount of static strain. Typical examples based on single test pieces are shown in Fig. 4 for newsprint. At 0.16% static strain, the storage modulus decreased 3% with increasing strain amplitude (0.005-0.100%). An increase to a plateau level in modulus can be seen at zero static strain when the strain amplitude was increased. The dissipation factor increases with the strain amplitude and the amount of static strain for the tested papers. The random error on $\tan\delta$ was reduced by increasing the strain amplitude. The signal output, independent of the strain amplitude and static strain, was never ideally linear. It was decided to set the strain amplitude to $\hat{\varepsilon} = 0.075\%$ for further trials.

At the selected condition, stationary responses were found in the range of frequencies tested. In Figs. 5, the in-plane dissipation factors $\tan\delta_{\alpha\beta}$ of newsprint are shown. All the dissipation factors were frequency dependent. This was especially pronounced at the lowest and highest frequencies for the papers tested.

The storage modulii are presented in Fig. 6. It can be seen that the storage properties exhibits only a small frequency dependence at this condition. The modulus G_{22}' which changes the most, increased 18% from 0.000238 to 10 Hz. The coupled storage modulii G_{12} and G_{21} were for the tested paper of the same order of magnitude over the whole frequency window. The stiffness anisotropy of the material was found to decrease at increasing frequency with 7% for the newsprint in the range of frequencies tested.

For the in-plane shear storage modulus $G_{66}'^{w}$ increasing frequency results in an increasing $G_{66}'^{w}$ similar to the other in-plane storage modulii. The increase was 15% from 0.000238 to 10 Hz.

The TE-algorithm was used on harmonic in-plane source data to obtain the in-plane line spectras of paperboard and newsprint. The cut-off frequencies were selected to be 10^{-4} and 10^{2} Hz and eleven terms ($N = 11$) were used in the summation.

Creep and creep recovery type of experiments were used to examine the flow behavior of paperboard. The material was subjected to a load stimuli in MD shown in Fig. 2a at two incremental specific stress levels $\Delta\sigma_{11}^{w} = 6$ and 12 kNm/kg. An example of this is shown in Fig. 7. It can be seen that the predicted creep curves underestimated the measurements in both nominal directions when loading in MD. The predictions were based on the in-plane storage compliances. Only small deviations were found on creep recovery at this load level independent of loading direction. When testing in CD larger deviations were found. At increasing load, the discrepancy between predictions and measurements increased. The errors of the predictions were about 10% except for loading in CD.

Relaxation experiments were performed on paperboard at different constant strain levels in MD. The longitudinal stress decay, and the transverse strain were measured during testing. All model predictions were based on the storage modulii. After one second of constant strain rate, the longitudinal strain were kept constant in time at 0.05, 0.10 or 0.20%. The results of simulations and measurements of stress decay are given in Fig. 8a where the response to the constant strain rate at the loading phase is included. Small deviations between predictions and measurements of stress decay were observed at the strain levels of 0.05 and 0.10%. At the high strain level, both the trend and the magnitude of the predicted stress decay differed from the measurements.

Predictions and measurements of the transverse strain response to the relaxation stimuli for two strain levels are given in Fig. 8b. As expected, the transverse strain exhibited shrinkage during the longitudinal straining period up to one second. Further transverse shrinkage was observed at increasing time when the longitudinal strain was kept constant.

Experiments were performed on both paperboard and newsprint in the MD according to the deformation history shown in Fig. 2b. A total cycle time of 100 seconds was chosen. An example of the newsprint stress response is shown in Fig. 9. The predicted stress response was in very good agreement over the entire strain cycle. The scatter in the results of the three replicates was as small.

DISCUSSION

In the experiments the pressure pulses arising from the glass plates during the compressive part of the stress strain cycle were neglected. These effects are, however, likely to be negligible when considering the limited coupling effect from the thickness direction to the in-plane behavior of paper. Furthermore, we neglected disturbances of the stress field from the clamps and the needles.

Small out-of-plane motions, i.e. buckling, were observed during testing. In compression, with plates at large clearances, we observed waves in the longitudinal direction. In tension, when the plates were removed, we observed that the test piece curled with its axis in the longitudinal direction. These out-of-plane motions were considered to be the sources for the problems during the measurements of the transverse motion at larger clearances between the test piece and the glass plates, i.e. in conditions when the loss angles could be determined. The low thickness to the in-plane dimension ratio of newsprint test pieces make them sensitive to these out-of-plane motions even at small disturbances. Thus, paper with higher thickness like paperboard reduces this phenomenon.

The fact that the computed signal noise from the experimental data was of the same magnitude as the true noise found on an oscilloscope guides the interpretation of accurate measurements. This was found to be an important way to check if the setup interfered with the measurements.

The results show that the paper grades tested exhibited anisotropic in-plane viscoelastic behavior. However the time dependence of the materials was rather small. The fact that test pieces loaded in CD exhibited a more pronounced frequency dependence than in MD explains the frequency dependence on the stiffness anisotropy. A time dependence on the anisotropy is shown during relaxation experiments on kraft sack paper by Uesaka *et al.* [2].

Our measurements show a large reduction in all the evaluated in-plane dissipation factors at 10 Hz. This result might be apparatus dependent. However similar reductions on the dissipation properties at higher frequencies is found by Luidl [11]. The beginning of a transitional region of the dissipation factors at lower frequencies was found for the tested papers.

A general interest was the conversion from the frequency to the time domain. The results show that the discrete harmonic experimental data was well reproduced by continuous functions created from parameters obtained by the TE-algorithm. Instead of using an interpolation routine to estimate data between the experimental values as used in the present work, the power of the TE-algorithm could be used on pure experimental data. In the present work, this would not have improved the model predictions to any great extent since the time dependence was limited and exhibited regular behavior of the materials at the tested conditions.

Paperboard and newsprint were subjected to different stimuli in order to examine the classic anisotropic linear viscoelastic model with material parameters obtained from source data found at the displacement controlled sinusoidal excitations. Some creep and creep recovery trials were selected to obtain longitudinal strains closely to those in the dynamical experiments. Despite this, a small systematic deviation, independent of loading and response directions, was found between prediction and measurement of the creep strains. A significant but small improvement of the creep and creep recovery strains prediction was shown when partly using the loss properties.

The paper grades tested were found to exhibit a small nonlinear behavior even at small strains below a strain amplitude of 0.10%. The source data [5], used here, describes likely a stiffer material since the signal processing used for their evaluation is likely to not capture nonlinearities of this kind and would explain the remaining systematic deviations. This was supported by the excellent performance observed during stress relaxation at the constant strain $\varepsilon_{11} = 0.05\%$. The deviation between predictions of creep in the longitudinal and the transverse directions compared to measurements were also found to increase at higher longitudinal stress levels.

The determination of small transverse strains on rectangular paper test pieces are affected with several experimental difficulties. First of all, at low σ_{22} stress levels the signal-to-noise ratio on the transverse strain signal was quite poor. In part, this explains why the model predictions of the transverse creep strains were improved at higher stress levels. Secondly, the non-uniformity of paper may cause substantial scatter in the determination of small transverse strains and demand more replicate tests.

The paper web is usually under velocity control when it passes through the printing units in an offset printing press. It is near a state of stress relaxation with some small hereditary effects from the preceding loading steps. In the present investigation, only small stress decays were found in relaxation measurements and simulations. At higher moisture contents this phenomenon will likely increase. The time dependent transverse strain at a constant longitudinal strain plays an important role in the understanding of misregister. Our measurements and model simulations showed an increasing transverse shrinkage with increasing time. Similar uniaxial predictions performed by Uesaka *et al.* [2] on hand made sheets regarded as transversally isotropic show the contradictory result that the transverse shrinkage decreased at increasing time.

The complex deformation history used in this work may be regarded as a simplified version of the web loading in a printing press at another time scale. In practice, the web passes through the printing press in a few seconds. The measurements followed closely the model response. Especially, newsprint showed excellent performance. The compressive stress immediately after unloading was an interesting observation. This was an effect of viscoelastic behavior of the materials. In the work of Guan *et al.* [1], the finite unloading time is neglected which may be a good approximation in web transport. A selection of cut-off frequency higher than 100 Hz in the procedure for the determination of material parameters ought to improve the prediction of the compressive stress peak.

Mechanical conditioning or immersion of paper in water are suggested treatments in order to reduce residual stresses. Neither of these preconditioning techniques were used on the papers tested. Still, the two-dimensional linear viscoelastic theory was found to work well at small strains and constant environmental conditions. It remains to investigate both uniaxial compressive and multiaxial stress states other than those produced by off-axis loading.

The measurements of recovery strains, independent of direction, indicated only limited irreversible flow. Irreversible flow has been found earlier, especially at higher stress levels than used in this work. Furthermore, transient effects from the water supplied under pressure and mechanical loading in combinations are other difficulties of interest when striving to understand the mechanics of running paper webs.

CONCLUSIONS

The robustness of a novel experimental method to evaluate in-plane viscoelastic properties of paper was shown. Stationary responses during dynamic testing in the frequency range 0.00024 to 10 Hz was obtained.

An ideal linear viscoelastic response of the tested papers was never found. However, below 0.1% in strain amplitude this nonlinearity was small. An anisotropic frequency dependence on the viscoelastic properties was found.

It was found that the linear model well described the behavior of newsprint and paperboard at loading adequate to printing conditions.

The time dependent transverse strain response of machine made paper due to stress relaxation and creep was demonstrated and should be considered in the analysis of running paper webs.

ACKNOWLEDGMENT

This work was carried out as a part of the Swedish interdisciplinary Print Research Program (PFT).

REFERENCES

1. Guan, X., High, M. S. and Tree, D. A., "Viscoelastic Effects in Modeling Web Handling Systems: Steady State Analysis," Journal of Applied Mechanics, Vol. 62, 1995, pp. 908-914.

2. Uesaka, T., Murakami, K. and Imamura, R., "Two-dimensional Linear Viscoelasticity of Paper," Wood Science and Technology, Vol. 14, 1980, pp. 131-142.

3. Uesaka, T., Murakami, K. and Imamura, R., "Anisotropic Linear Viscoelasticity of Paper Sheet," Journal Society of Rheology Japan, Vol. 7, 1979, pp. 64-68.

4. Tschoegl, N. W., The Phenomenological Theory of Linear Viscoelastic Behavior: An Introduction, Springer-Verlag, Berlin, Heidelberg, 1989.

5. Lif, J.O., "Experimental methods and time dependent characterization of paper for printing applications," ISRN KTH/HFL/LA--56--SE, 1997, Department of Solid Mechanics, Royal Institute of Technology, S-100 44, Stockholm, Sweden.

6. Akatsuka, M., "Models of Longitudinal Web Behavior Incorporating Viscoelasticity," Mitsubishi Heavy Industry Ltd Technical Review, Vol. 29, No. 1, 1992, pp. 44-48.

7. Emri, I. and Tschoegl, N. W., "Generating Line Spectra from Experimental Responses. III. Interconversion between Relaxation and Retardation Behaviour, International Journal of Polymeric Materials, Vol. 18, 1992, pp. 117-127.

8. Emri, I. and Tschoegl, N. W., "Generating Line Spectra from Experimental Responses. Part I: Relaxation Modulus and Creep Compliance," Rheological Acta, Vol. 32, 1993, pp. 311-321.

9. Emri, I. and Tschoegl, N. W., "Generating Line Spectra from Experimental Responses. Part IV: Application to Experimental Data," Rheological Acta, Vol. 33, 1994, pp. 60-70.

10. Tschoegl, N. W. and Emri, I., "Generating Line Spectra from Experimental Responses. Part II: Storage and Loss Functions," Rheological Acta, Vol. 32, 1993, pp. 322-327.

11. Luidl, C., "Kenngrössen von Endlospapieren," Forshungsbericht Nr. 66.006, (1994), FOGRA, München, Germany.

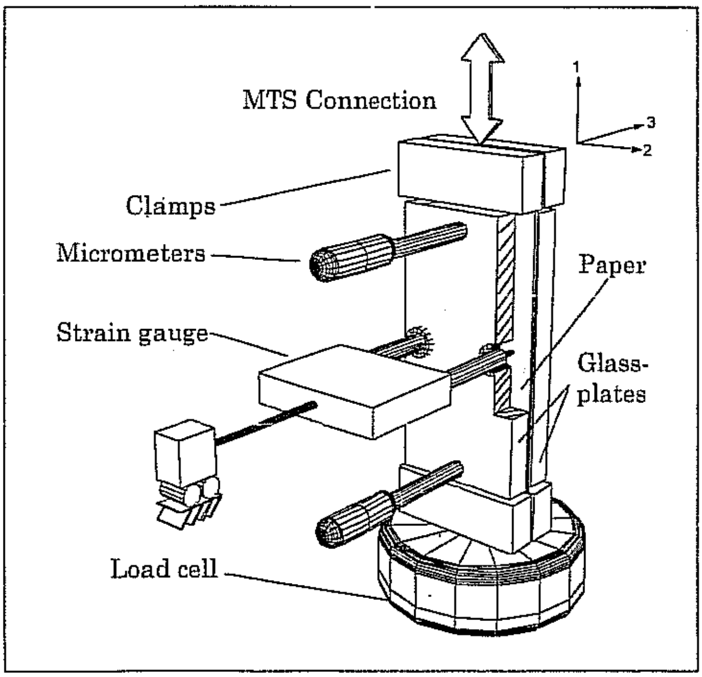

Fig. 1 The in-plane deformation tester.

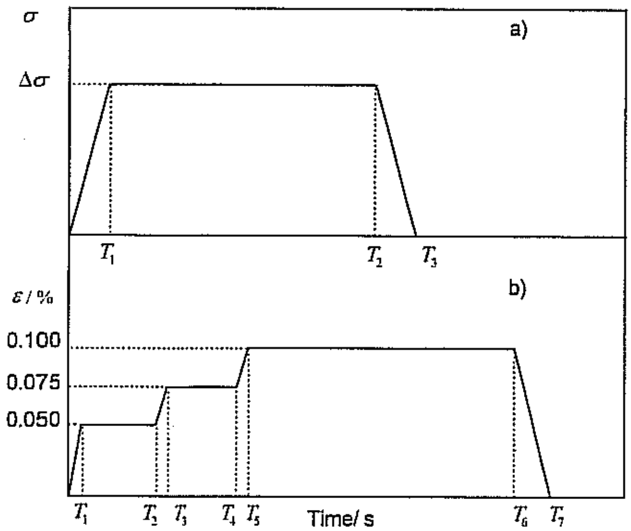

Fig. 2 **Loads in the time domain: a) The creep and creep recovery excitation and b) the complex strain history.**

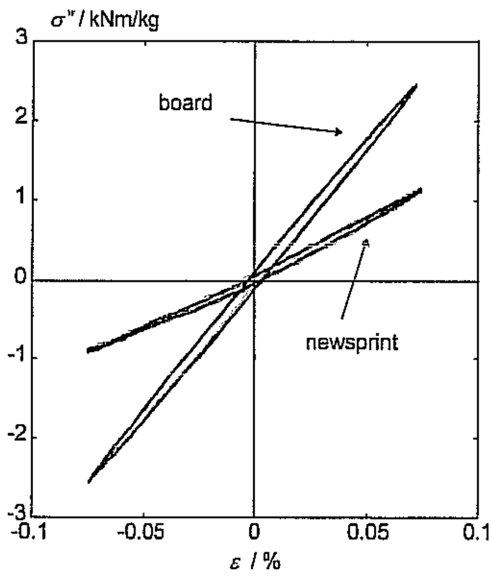

Fig. 3 **The stress response to sinusoidal strain excitation on newsprint and paperboard loaded in CD. Experiments at 0.075% strain amplitude, at a frequency 0.000236 Hz and a clearance of 0.05 mm. The total cycle time is 14 hours.**

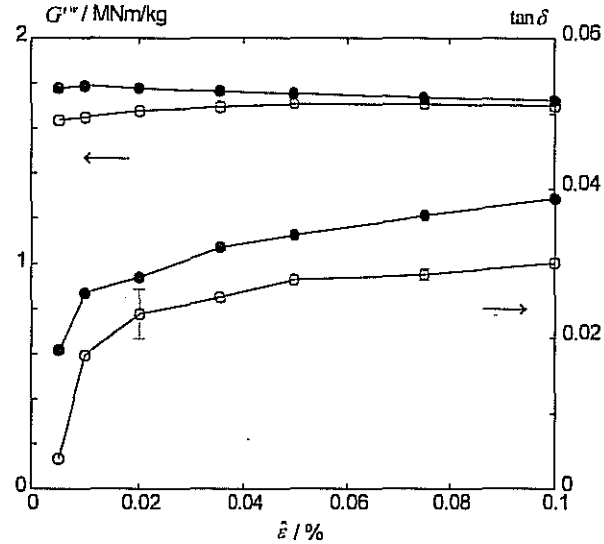

Fig. 4 **Examination of the linearity of newsprint. G'^{W} and $\tan\delta$ determined at zero (○) and 0.16% static strain (●) at a frequency of 1 Hz and with loading in CD. Note the estimated random error.**

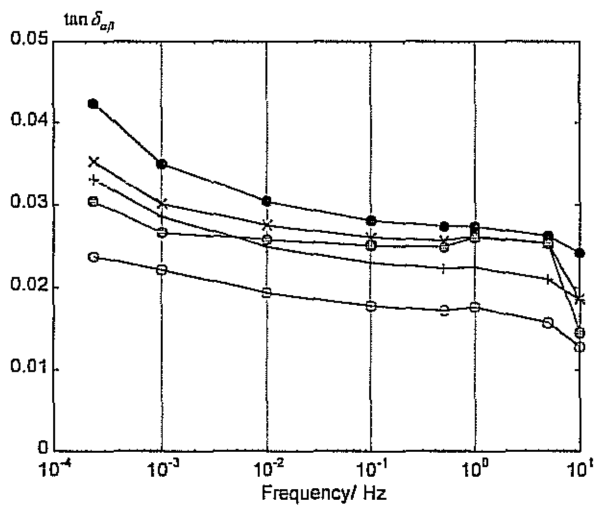

Fig. 5 **In-plane dissipation factors of newsprint. In-plane dissipation factors of newsprint. $\tan\delta_{11}$ (○), $\tan\delta_{22}$ (●), $\tan\delta_{12} = \tan\delta_{21}$ (+), $\tan\delta_{45}$ (×) $\tan\delta_{66}$ (⊕).**

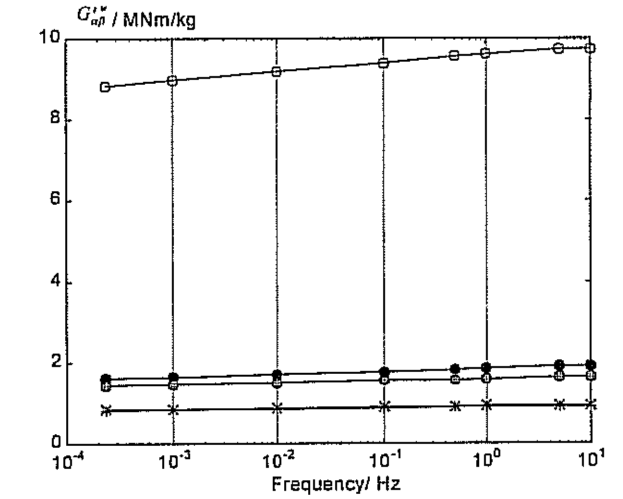

Fig. 6 **In-plane storage modulii of newsprint.** G_{11}' (○), G_{22}' (●), G_{12}' (+), G_{21}' (×) **and** G_{66}' (⊕).

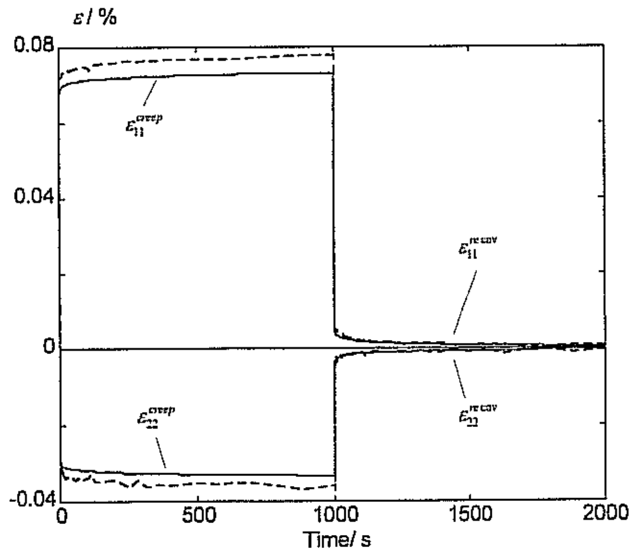

Fig. 7 **Creep and creep recovery of paperboard. The incremental specific stress level is** $\Delta\sigma_{11}^{w}$**=6 kNm/kg. The solid lines represent the predictions and the dashed lines are the measurements.**

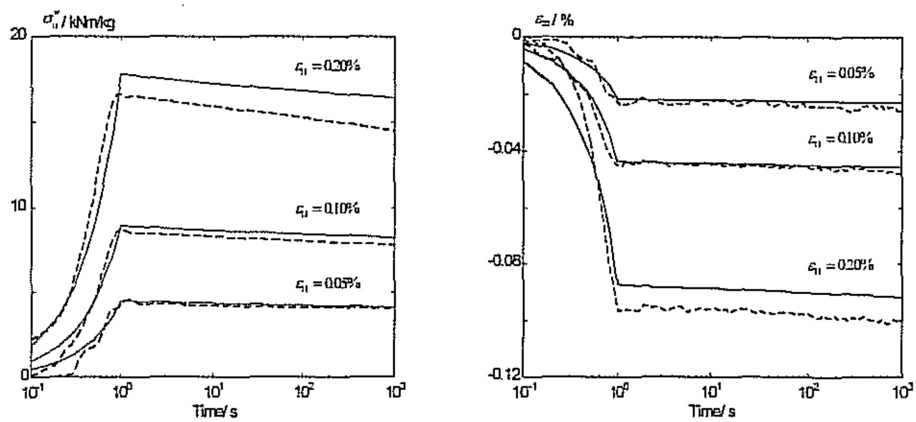

a) b)

Fig. 8 **a) Stress relaxation of paperboard.**
b) The transverse strain response during relaxation of paperboard. The solid lines represent the predictions and the dashed lines are the measurements.

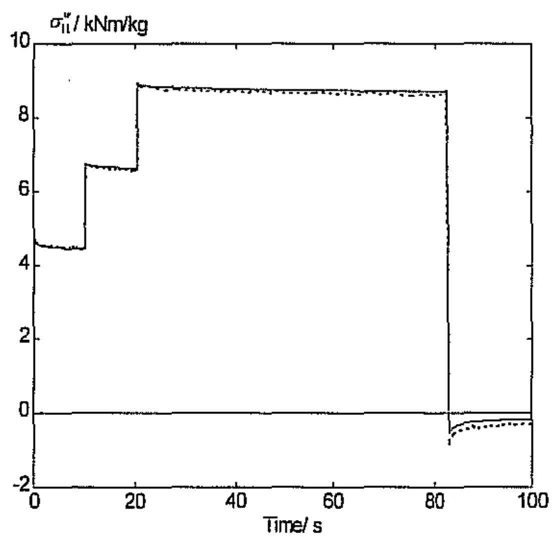

Fig. 9 **The specific stress response of newsprint to the deformation history in Fig. 2b. The solid line represents the prediction and the dashed line is the measurement.**